Abrogation of Protein Uptake through Megalin-Deficient Proximal Tubules Does Not Safeguard against Tubulointerstitial Injury

Franziska Theilig,* Wilhelm Kriz,† Timo Jerichow,* Petra Schrade,* Brunhilde Hähnel,† Thomas Willnow,‡ Michel Le Hir,§ and Sebastian Bachmann*

*Institute of Anatomy, Charité Universitätsmedizin, and ‡Max-Delbrück-Center for Molecular Medicine, Berlin, and †Zentrum für Medizinische Forschung, Mannheim, Germany; and §Institute of Anatomy, University of Zurich, Zurich, Switzerland

Sustained proteinuria and tubulointerstitial damage have been closely linked with progressive renal failure. Upon excess protein endocytosis, tubular epithelial cells are thought to produce mediators that promote inflammation, tubular degeneration, and fibrosis. This concept was tested in a transgenic mouse model with megalin deficiency. Application of an anti–glomerular basement membrane serum to transgenic megalin-deficient mice [Cre(+)/GN] and megalin-positive littermates [Cre(−)/GN] produced the typical glomerulonephritis (GN) with heavy proteinuria in both groups. Tubulointerstitial damages correlated closely with glomerular damages in pooled Cre(+)/GN and Cre(−)/GN mice. Owing to a mosaic pattern of megalin expression in the mutant mice, Cre(+)/GN kidneys permitted side-by-side analysis of megalin-deficient and megalin-positive tubules in the same kidney. Protein endocytosis was found only in megalin-positive cells. TGF-β, intercellular adhesion molecule, vascular cellular adhesion molecule, endothelin-1, and cell proliferation were high in megalin-positive cells, whereas apoptosis, heat-shock protein 25, and osteopontin were enhanced in megalin-deficient cells. No fibrotic changes were associated with either phenotype. Tubular degeneration with interstitial inflammation was found only in nephrons with extensive crescentic lesions at the glomerulotubular junction. In sum, enhanced protein endocytosis indeed led to an upregulation of profibrotic mediators in a megalin-dependent way; however, there was no evidence that endocytosis played a pathogenetic role in the development of the tubulointerstitial disease.

J Am Soc Nephrol 18: 1824–1834, 2007. doi: 10.1681/ASN.2006111266

ESRD is defined by an irreversible decline of renal function. In most cases, the disease starts in the glomerulus and is then transferred to the tubulointerstitium. Concerning this transfer, two major hypotheses, although not necessarily mutually exclusive, are under discussion. One is focused on the glomerular damage as the presumptive central event, causing obstruction of the initial nephron segment and consecutive degeneration of the tubule ("glomerular hypothesis" [1]). The other, commonly assumed hypothesis refers to the loss of glomerular permselectivity and consequent protein leakage into the tubular fluid, followed by excessive protein reabsorption by the proximal tubule. Under these conditions, proximal tubule cells are thought to produce a variety of inflammatory mediators that induce peritubular inflammation, tubular damage, and fibrosis ("tubular hypothesis" [2–6]).

Protein reabsorption by the proximal tubule involves binding to megalin, a 600-kD transmembrane glycoprotein that belongs to the LDL receptor gene family. Megalin has been introduced as the key molecule for the uptake of all major proteins that are increased in proteinuria (7,8).

Studies in animal models and cell culture systems have shown that protein overload on renal tubules leads to the expression of inflammatory and profibrotic products (9–12). However, both approaches are hampered by common drawbacks, such as the difficulty in animal models to identify links of causality between the various altered parameters and the reductionist nature of the isolated cell system. We have made use of a transgenic mouse model with kidney-specific megalin deficiency to study the role of tubular endocytosis in degenerative renal damage (13). Megalin-deficient kidneys exhibit massive reduction in proximal tubular endocytosis, resulting in low molecular weight proteinuria. A key feature of this model, the mosaic remnant expression of megalin in a subset of proximal nephrons (20 to 40% [14]), first seemed to be an obstacle for the interpretation of our results but actually turned out to be a major advantage that allowed us to compare the responses to protein overload in neighboring megalin-positive and megalin-deficient cells.

We induced glomerulonephritis (GN) in these mice and controls to test the hypothesis that excessive protein uptake by proximal tubule cells may lead to tubulointerstitial damage. Morphologic changes and the expression of inflammatory and

Received November 22, 2006. Accepted March 12, 2007.

Published online ahead of print. Publication date available at www.jasn.org.

Address correspondence to: Prof. Sebastian Bachmann, Charité, Universitätsmedizin Berlin, Institut für Vegetative Anatomie, Philippstrasse 12, 10115 Berlin. Phone: +49-30-450-528-001; Fax: +49-30-450-528-922; E-mail: sbachm@charite.de

Copyright © 2007 by the American Society of Nephrology

ISSN: 1046-6673/1806-1824

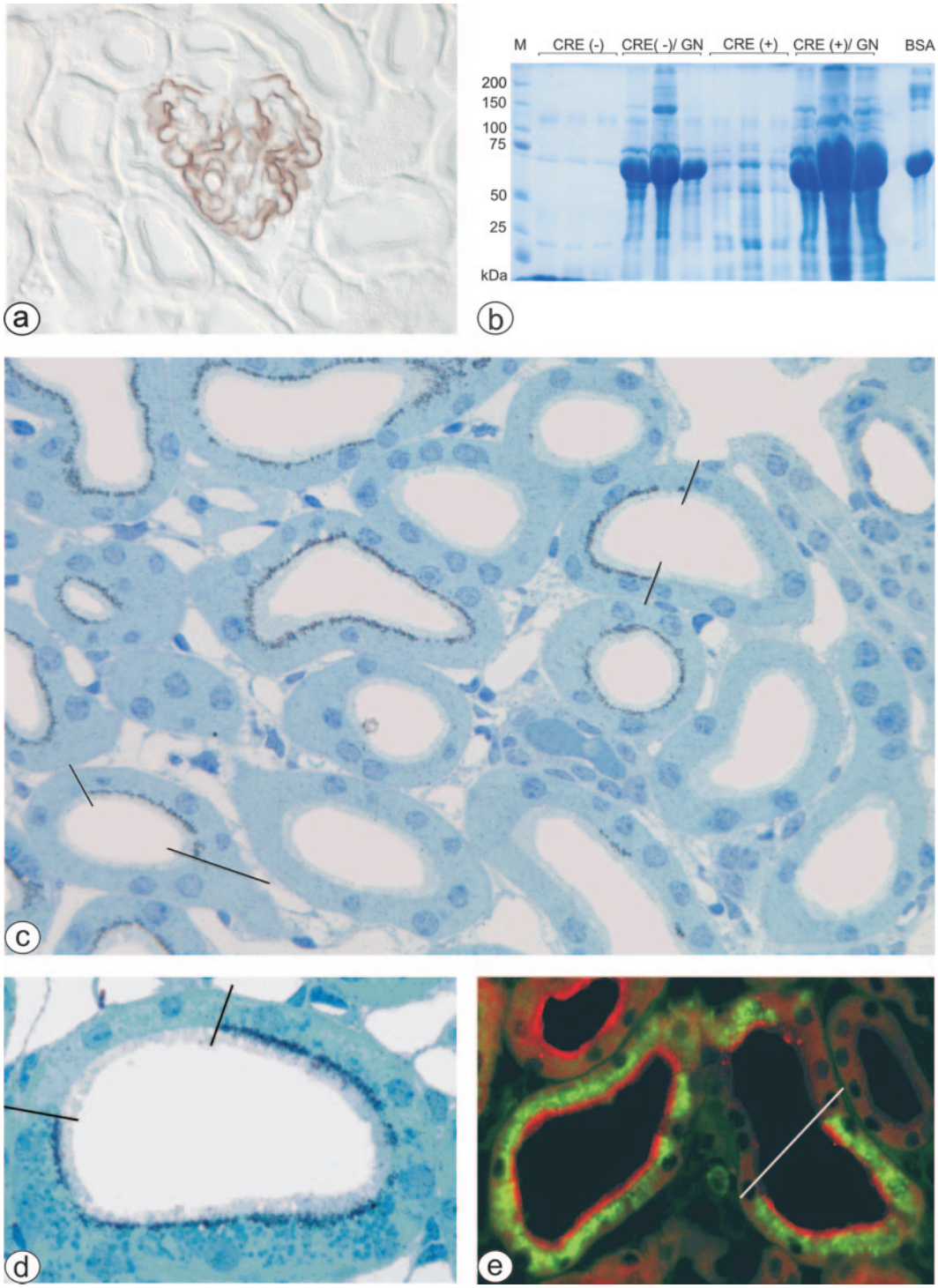

Figure 1. Characterization of Cre(−) and Cre(+) mice 18 d after the induction of glomerulonephritis (GN). (A) Immunostaining of glomerular basement membrane (GBM) deposits with horseradish peroxidase–coupled anti-rabbit IgG. (B) Coomassie staining of urinary proteins. M is the marker for protein size; BSA serves as positive control. Compared with Cre(−) mice, Cre(+) mice show a low molecular weight proteinuria with major bands at the BSA level. Cre(+) mice with GN [Cre(+)/GN] show markedly elevated proteinuria compared with Cre(−) mice with GN [Cre(−)/GN]. (C) Immunogold-silver staining for megalin in an overview of a Cre(+) control kidney. The black silver deposit at the basis of the microvilli identifies cells with remnant megalin expression; semithin section stained with Richardson's blue. Bars indicate borders between megalin-positive and megalin-deficient cells. (D) Cre(+)/GN kidney, staining as in C; intracellular blue dots reveal massive uptake of filtered proteins, which is visible only in megalin-positive cells. (E) Double immunostaining of mouse IgG (green fluorescence) and megalin (red fluorescence) in Cre(+)/GN cryosection. IgG uptake is strictly co-localized with megalin. Bar indicates the border between a megalin-positive and a megalin-deficient epithelial portion. Magnifications: ×250 in A; ×200 in C; ×800 in D; ×300 in E.

cell-cycle parameters were comparatively analyzed in megalin-expressing cells with intensive protein endocytosis and in megalin-deficient cells with compromised endocytosis. Our results provide important new information with respect to the validation of the "glomerular hypothesis" as compared with the "tubular hypothesis."

Materials and Methods

Animals and Treatments

Experiments were performed in adult female, kidney-specific, Cre-positive megalin knockout mice (megalin lox/lox; apoE Cre), here termed Cre(+), and in Cre-negative control mice (megalin lox/lox), termed Cre(−) (13,14). The extent of megalin gene deletion in the proximal epithelia of Cre(+) naturally varied to substantial amounts, thereby determining variability in the degree of basal proteinuria. For preselection of suitable mice, the degree of remnant megalin expression in Cre(+) was therefore estimated by sampling of urinary levels of vitamin D–binding protein (13). For further assessment of the megalin status in mice that were selected for histologic analysis, a rate of 60 to 80% of megalin-deficient proximal tubule profiles (PTP) was standardized immunohistochemically. A total of 24 pooled littermates [Cre(+) and Cre(−) mice] from several litters were used. Twelve Cre(+) and 12 Cre(−) mice were immunologically primed by subcutaneous injection of rabbit IgG in complete Freund's adjuvant. GN was induced 6 d later by the intravenous injection of an anti-mouse glomerular basement membrane (GBM) serum (15) in eight Cre(+) and eight Cre(−) mice, whereas four mice of each genotype received an injection of vehicle (0.9% NaCl). During treatment, mice were allowed free access to standard diet and tap water. Another 18 d later, all mice were killed. For urinalysis, mice were individually placed in metabolic cages for 24 h between day 0 and day 6 and on the last day before being killed. Urine protein and creatinine concentration were determined (kits from Roche Diagnostics, Mannheim, Germany). Urine was electrophoresed using BSA as a standard. The experiments were conducted in accordance to the German law for the protection of animals (Registered under G 0178/03).

Morphologic and Cytochemical Preparations

Mice were anesthetized by an intraperitoneal injection of sodium pentobarbital (0.06 mg/g body wt), and the kidneys were perfusion-fixed using 3% paraformaldehyde and prepared for light microscopy and electron microscopy analysis (14,16).

Periodic acid-Schiff–stained paraffin sections were used for scoring analyses. Semithin plastic sections (1 μm) were serially sectioned and stained with Richardson solution; several series from tissue blocks of Cre(+) and Cre(−) were cut, and the relevant glomeruli were selected in the midst of a series and traced toward both sides. Ultrathin sections were contrasted with uranyl acetate and lead citrate. Immunolabeling was performed on cryostat or paraffin sections or on semithin LR white-plastic sections. As primary antibodies, sheep anti-megalin (gift from P. Verroust, INSERM U538, Paris, France), guinea pig anti-megalin (generated against the c-terminus of rat megalin), rat anti–intercellular adhesion molecule-1 (anti–ICAM-1; clone KAT-1; ImmunoKontact, Abingdon, UK), rat anti–vascular cellular adhesion molecule-1 (anti–VCAM-1; BD Transduction, Heidelberg, Germany), rabbit anti–heat shock protein 25 (anti–HSP25; Calbiochem, Schwalbach, Germany), rabbit anti–collagen I (Research Diagnostics Natu-Tec, Frankfurt, Germany), rat anti-CD68 (Serotec, Düsseldorf, Germany), rabbit anti–α-smooth muscle actin (Abcam, Cambridge, UK), goat anti-vimentin (Sigma, Taufkirchen, Gernamy), rabbit anti–monocyte chemoattractant protein-1 (anti–MCP-1; Santa Cruz Biotechnology, Santa Cruz, CA), rabbit anti-PCNA (Santa Cruz Biotechnology), rat anti–Ki-67 (Dako, Hamburg, Germany), or rabbit anti-S100A4 (Dako) were used. Suitable cy2- or cy3-coupled (Dianova, Hamburg, Germany) or horseradish peroxidase–coupled (Dako) secondary antibodies were applied. Horseradish peroxidase signal was generated with diaminobenzidine added with H_2O_2. For megalin immunostaining of semithin sections, 12 nm of colloidal gold–coupled anti-sheep antibody was used in combination with IntenSE-silver enhancement system (Amersham, Freiberg, Germany). For double immunostaining, various primary antibodies were administered consecutively. Specificity controls were done as described previously (14).

TGF-β1, TGF-β3, osteopontin, and endothelin-1 (ET-1) mRNA expression was studied by *in situ* hybridization using digoxigenin-labeled riboprobes (Roche). Sense and antisense probes were generated by *in vitro* transcription of a 500-bp TGF-β1, a 500-bp TGF-β3, an 1100-bp osteopontin, and a 300-bp ET-1 cDNA template. *In situ* hybridization was performed on paraffin sections and combined with immunohistochemistry as described previously (16). For detection of DNA fragmentation, terminal deoxynucleotidyl transferase–mediated digoxigenin-deoxyuridine nick-end labeling (TUNEL) staining was performed using an *In Situ* Cell Death Detection Kit (Roche). A Leica DMRB fluorescence microscope equipped with a digitized camera system and MetaView software (Visitron, Puchheim, Germany) and a Zeiss EM 906 were used for evaluation.

Quantifying Assessments

A semiquantitative score of the glomerular and tubulointerstitial damage was established as described previously (17). For assessment of inflammatory parameters, stress proteins, and apoptosis, sections that were double immunostained with megalin and ICAM-1, TGF-β1, TGF-β3, ET-1, osteopontin, MCP-1, or HSP25 were evaluated by counting of megalin-positive and/or megalin-deficient PTP, respectively, for the simultaneous presence or absence of these parameters. Megalin half-positive *versus* half-negative PTP portions were separately assigned. VCAM-1, PCNA, Ki-67, and TUNEL signals were evaluated by single

Table 1. Clinical data[a]

Parameter	Cre(−)/Control	Cre(+)/Control	Cre(−)/GN	Cre(+)/GN
Body weight (g)	29.63 ± 2.75	29.13 ± 1.86	22.53 ± 5.07	24.60 ± 3.38
Urine volume (ml/d)	0.47 ± 0.11	0.75 ± 0.43	1.56 ± 0.43[b]	2.21 ± 0.22[b,c]
Urinary protein excretion (mg/d)	1.57 ± 0.20	2.73 ± 0.79	8.28 ± 3.39[b]	28.84 ± 10.14[b,c]
Urine protein/urine creatinine	4.64 ± 0.36	6.84 ± 1.69	19.78 ± 5.19[b]	73.80 ± 21.92[b,c]

[a]Data are means ± SD. Groups with glomerulonephritis (GN) are compared with the respective control groups.
[b]$P < 0.05$, control *versus* GN.
[c]$P < 0.05$, Cre(−) *versus* Cre(+).

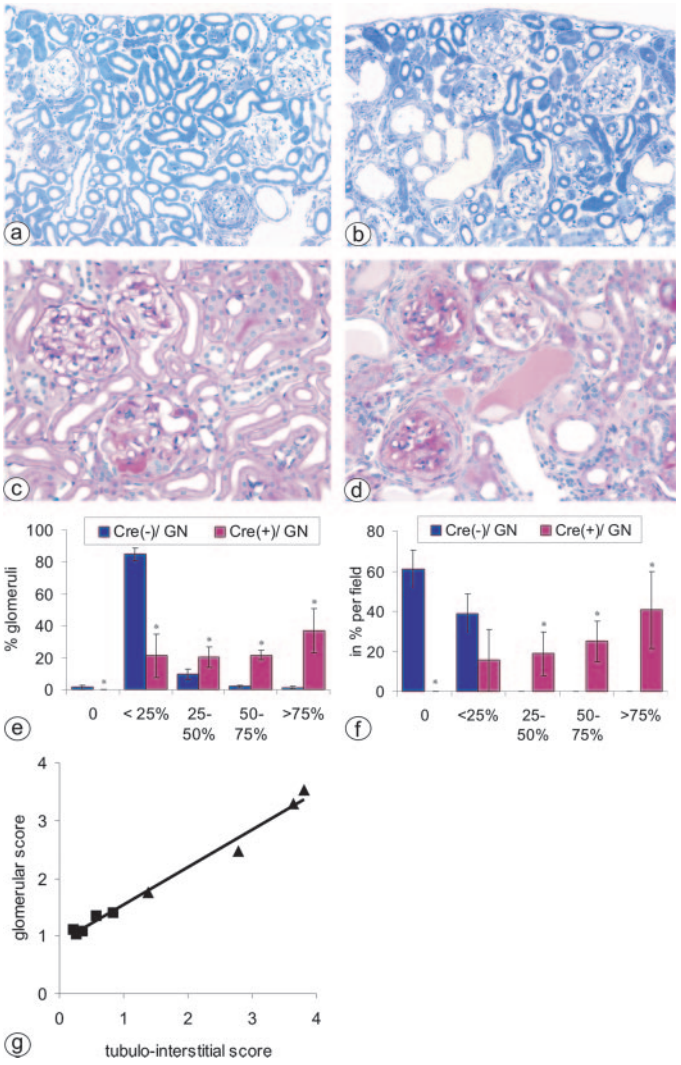

Figure 2. Histopathologic characterization. (A and B) Overview of kidney cortex of a representative Cre(−)/GN (A) *versus* Cre(+)/GN kidney (B). Inflammation, glomerulosclerosis, obstruction or dilation of tubules, and tubulointerstitial fibrosis have evolved in Cre(−)/GN tissue but are much more pronounced in Cre(+)/GN (semithin sections). (C and D) Glomerulosclerosis and inflammatory detail as revealed by periodic acid-Schiff staining in representative Cre(−)/GN (C) *versus* Cre(+)/GN mice (D) on paraffin sections as used for damage scoring. (E and F) Tissue damage, given as percentage changes of the glomeruli (E) and of the tubulointerstitium per optical field (F) according to the respective ranges of scores from Cre(−)/GN and Cre(+)/GN mice. Data are means ± SD. *$P < 0.05$. (G) Correlation between damage scores of the pooled groups. Linear regression line with r indicating linear correlation coefficient. Magnifications: ×80 in A and B; ×100 in C and D.

cell counts. Five mice per group were evaluated throughout. Ultrastructural parameters of proximal tubules were estimated from 100 electron micrographs per kidney ($n = 4$ mice per group). Megalin-positive cells were distinguished from megalin-deficient cells using structural criteria (14). Cell height, microvillar length, and tubular basement membrane thickness were determined by calculation of the means of three individual measurements per cell performed at random. The mitochondrial and lysosomal contents of tubular cells were estimated by stereology (18) using the MetaVue analyzing software (MetaVue, München, Germany).

Statistical Analyses

Data were analyzed using SPSS statistic program (SPSS, Chicago, IL). Quantitative data are presented as means ± SD. For statistical comparison, the Mann-Whitney rank sum test was used. For the assessment of correlation, the Pearson test was used. $P < 0.05$ was considered statistically significant.

Results

GN and Megalin-Deficient Mice

Application of the nephritogenic antibody to Cre(−) and Cre(+) mice induced GN with prominent proteinuria as established previously (15,19). Immunohistochemical detection of the nephritogenic antibody that bound to the GBM demonstrated specificity of the GN (Figure 1A). The entire kidneys of either genotype were affected, albeit with higher damage and proteinuria occurring in Cre(+) compared with Cre(−) mice (Table 1). This was confirmed by urine electrophoresis showing elevated baseline protein levels in Cre(+) mice owing to the expected low molecular weight proteinuria (Figure 1B) (13) and disproportionate enhancement of proteinuria in Cre(+) mice with GN. Most of the urine protein in GN was concentrated at the albumin level (Figure 1B).

Megalin deficiency in Cre(+) mice was incomplete. Previous studies using urinary excretion of vitamin D–binding protein as an indicator for the degree of megalin deficiency showed that knockout among PTP ranged between 60 and 80% (13). In our mice, an average of 69.8 ± 5.5% of all PTP were megalin-deficient as revealed by immunohistochemical quantification (Figure 1C). The presence or absence of megalin immunoreactivity in the brush border membrane (BBM) and underlying endocytic compartment was clearcut (Figure 1C). Uptake of filtered proteins in PTP or single cells with remnant megalin expression was visualized immunohistochemically (Figure 1, D and E). Numerically, 79.1 ± 13.2% of megalin-positive PTP showed uptake, whereas all megalin-deficient PTP were negative.

Histopathology of the Kidneys under Partial Megalin Deficiency and Proteinuria

Both treated groups developed crescentic GN with tubulointerstitial disease 18 d after injection of the anti-GBM serum. The histopathologic changes were qualitatively identical in both groups but quantitatively more pronounced in Cre(+) than in Cre(−) mice (Figure 2, A through D). Glomeruli exhibited severe tuft alterations and cellular crescent formation (Figures 3, A and B, and 4). Tubulointerstitial damage presented with proximal tubular dilation and cast formation (Figure 2B) but also with atrophy, degeneration, and collapse (Figure 4, A and B). Vivid inflammation with peritubular hypercellularity and matrix deposition was encountered adjacent to the degenerating tubules (Figure 4, B and D). The degree of sclerotic, inflammatory, and degenerative damage was substantially higher in Cre(+)/GN compared with Cre(−)/GN (Figure 2, E and F). However, a strict, linear correlation ($r = 0.992$, $P < 0.001$) was

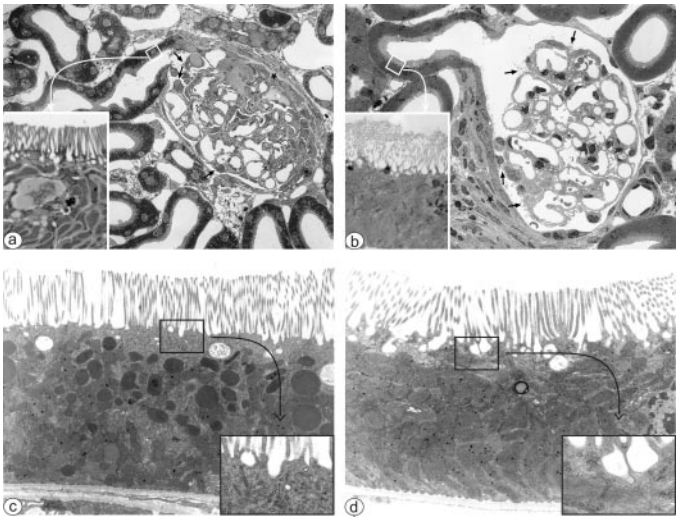

Figure 3. Electron microscopy. (A and B) Glomeruli from Cre(−)/GN (A) and Cre(+)/GN kidneys (B). Both glomeruli show inflammatory changes such as microvillous transformation (arrows) and crescent formation (star). In favor of demonstrating the initial tubular segment, in B, tuft adherence is not contained in this section plane but was identified by serial sectioning in this glomerulus as well. Both glomeruli reveal intact initial tubular segments. Enlarged inserts show the presence (A) or absence (B) of an endocytic apparatus, identifying this portion as megalin-positive (A) or megalin-deficient (B). (C and D) Proximal tubule cells derived either from megalin-positive (C) or megalin-deficient S1 segments (D) of a Cre(+)/GN kidney. Again, inserts illustrate presence (C) or absence (D) of the endocytic apparatus. Numerous primary and secondary lysosomes are present in C but not in D. Magnifications: ×450 in A and B; ×4600 in C and D.

found between the glomerular and the tubulointerstitial damage scores (Figure 2G).

Details of the glomerular changes and related consequences for tubule morphology were analyzed in serial sections tracing the glomerulotubular junctions and adjacent tubular profiles of affected glomeruli in Cre(+) and Cre(−) mice with GN. In GN, the initial proximal tubule was intact as long as there was no major encroachment of crescents from affected glomeruli (Figure 3, A and B). An entry of crescents into glomerulotubular transition, however, resulted in tubular degeneration, as detailed previously (19,20) (Figure 4, C through F). Further encroachment of the crescents was associated with collapse and obstruction of the tubule. Peritubular inflammation was restricted to the vicinity of collapsed segments, whereas unaffected nephrons that extended into areas of tubulointerstitial damage had maintained an intact structure (Figure 4D).

Ultrastructural Features of Proximal Tubular Changes Relative to Megalin Expression

Tubules from glomeruli that revealed crescent formation but not obstruction of the glomerulotubular junction were analyzed. Both glomeruli and tubules ranged within intermediate damage scores (>25 and <75%; Figure 2, E and F). The respective tubular cells, however, lacked destructive changes such as

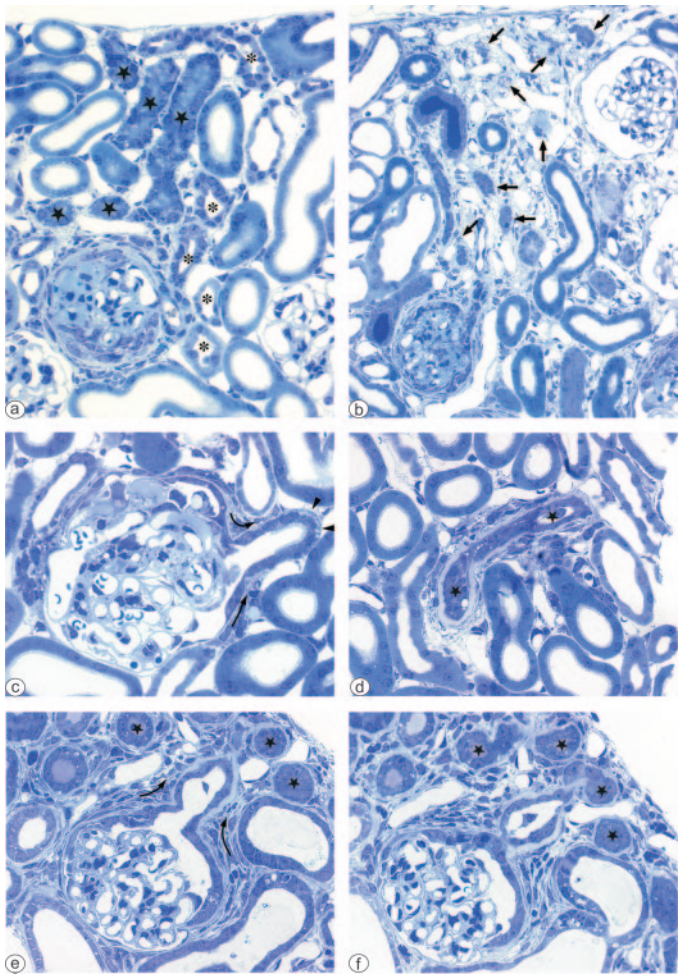

Figure 4. Representative images from semithin serial sectioning of kidneys from Cre(−) (A) and Cre(+) mice (B through F) with GN. Glomeruli show extensive crescents, and the connections to the tubule are obstructed as traced by serial sectioning (A and B). In A, the proximal tubules that belong to the collapsed glomerulus are fully collapsed (stars) and the distal tubules are narrowed (*). Interstitial inflammation is moderate. In B, all tubule profiles that belong to the collapsed glomerulus are atrophied with their remnants surrounded by inflammation and widened capillaries. In both A and B, tubules from neighboring nephrons do not seem to be affected by the inflammatory process. (C) Detail shows an inflamed glomerulus with encroachment of the crescentic process onto the first segment of the proximal tubule (arrows), revealing intercellular clefts (arrowheads; a sign of early damage [19]). The adjacent tubulointerstitium is normal. (D) Inflammatory reaction surrounding an atrophied profile (stars) that belongs to a massively damaged glomerulus. It is surrounded by a severe inflammatory response. Note that the inflammatory response does not affect the adjacent structures. (E and F) Affected glomerulus with encroachment of the crescentic inflammation toward the tubule *via* the glomerulotubular junction (arrows in E). The epithelium of the initial tubular segment is atrophied. Its lumen is patent, whereas downstream segments (stars; continuity shown in F) are collapsed as part of local, severe tubulointerstitial inflammation. Magnification, ×300.

cellular atrophy, dedifferentiation, and autophagy, which could have resulted from the exaggerated protein load (Figure 3, C and D). Apart from the general, drastic reduction of the endosomal apparatus in megalin-deficient cells, resulting in their moderately decreased cell height, specific GN-related differences were registered among groups in megalin-positive *versus* megalin-deficient cells with respect to total cell and brush border height, mitochondrial volume, and tubular basement membrane thickness. Predictably, lysosomes displayed major changes selectively in the megalin-positive cells (Table 2).

Histochemical Evaluation of Parameters Related to Inflammation and Cell Cycle

The expression of proteins whose upregulation was shown earlier in tubulointerstitial inflammation and of parameters related to the cell cycle were quantitatively compared in megalin-deficient *versus* megalin-expressing PTP of Cre(+)/GN mice. Control Cre(+) and Cre(−) mice as well as Cre(−)/GN mice were compared on a qualitative level.

ICAM-1 and VCAM-1. In control tissues, ICAM-1 was only faintly expressed in the BBM of a few single proximal tubule cells and in capillary endothelia, whereas VCAM-1 was not detectable. In Cre(+)/GN, ICAM-1 was upregulated predominantly in the BBM of megalin-positive PTP; with a similar distribution, VCAM-1 was upregulated in the basolateral cell aspect (Figures 5, A and B, and 8A). These changes were also found in Cre(−)/GN. Data suggest that an upregulation of the inflammatory adhesion molecules ICAM-1 and VCAM-1 is associated with enhanced protein endocytosis.

TGF-β. TGF-β1 and TGF-β3 were localized by *in situ* hybridization. No TGF-β signal was detected in control tissues. GN caused elevated expression of both cytokines in the glomeruli, proximal, and distal tubules of Cre(−) and Cre(+) kidneys. In Cre(+)/GN kidneys, expression of TGF-β1 and TGF-β3 was distinctly higher in megalin-positive than in megalin-deficient PTP (Figures 5, C through F, and 8), suggesting a link to endocytosis as well.

ET-1. The mRNA of this proinflammatory peptide was constitutively expressed in the distal tubule of control kidneys, whereas in GN, glomerular, interstitial, and proximal and distal tubular expression was induced. In Cre(+)/GN kidneys, megalin-positive PTP more frequently expressed ET-1, than megalin-deficient PTP (Figures 5, G and H, and 8).

Osteopontin and HSP25. The stress-related cytokine osteopontin was mainly expressed in medullary collecting ducts of control kidneys. In GN, osteopontin mRNA signal was strong in glomeruli and proximal and distal tubules; in contrast to the findings listed previously, however, in Cre(+)/GN, megalin-deficient PTP were more frequently osteopontin mRNA-positive than megalin-positive PTP (Figures 6, A and B, and 8). The stress protein HSP25 was strongly induced in glomeruli and proximal nephron segments and, to a lesser extent, in the distal tubules of GN kidneys. As for osteopontin, in Cre(+)/GN, a major share of the megalin-deficient PTP was strongly positive for HSP25 compared with the megalin-positive PTP (Figures 6C and 8).

MCP-1. This major inflammatory chemokine of tubular cells was apically present in proximal and distal tubules of Cre(+)/GN kidneys irrespective of megalin expression. It seemed that MCP-1 expression positively correlated with the individual nephron damage but was unrelated to cellular megalin expression (data not shown).

Apoptosis/Regeneration. For testing whether increased protein endocytosis had influenced epithelial cell cycle, proliferation (Ki-67 and PCNA) and apoptosis markers (TUNEL) were applied and the results were quantified in Cre(+) control and Cre(+)/GN mice. Baseline levels in controls showed an upregulation of all parameters in megalin-deficient cells (Table 3). Parameters were further increased substantially in GN, with more pronounced proliferation levels in the megalin-positive cells and higher apoptosis levels in the megalin-deficient cells (Figures 7 and 8, Table 3).

Peritubular Interstitium. Collagen I– and CD68-positive fibroblasts were diffusely enhanced in GN mice, with accumulations in the fibrotic interstitium surrounding degenerating tubule profiles whose epithelia were not principally free of remnant megalin expression. Searching across coronary kidney sections for an immediate spatial vicinity of megalin-positive *versus* megalin-deficient tubule portions and underlying positive fibroblasts, we could not detect a preferential association of the labeled fibroblasts with one or the other phenotype (Figure 9). Thus, there was no

Table 2. Numerical evaluation of structural parameters, proximal tubule[a]

Parameter	Epithelial Height (μm)	Brush Border Height (μm)	Basement Membrane Thickness (μm)	No. of Microvilli per μm	Primary/Early Secondary Lysosomes (%)	Late Secondary Lysosomes (%)	Mitochondria (%)
Cre(+)/control, megalin positive	5.73 ± 0.35	2.33 ± 0.34	0.08 ± 0.02	9.92 ± 1.50	1.77 ± 0.31	3.64 ± 1.79	42.04 ± 5.53
Cre(+)/control, megalin deficient	5.50 ± 0.81	2.31 ± 0.46	0.09 ± 0.02	10.39 ± 0.97	0.79 ± 0.22[b]	1.36 ± 0.53[b]	46.44 ± 8.41
Cre(+)/GN, megalin positive	7.64 ± 0.56[c]	2.16 ± 0.18	0.16 ± 0.04[c]	8.52 ± 0.98	11.08 ± 2.19[c]	9.51 ± 2.67[c]	22.89 ± 3.12[c]
Cre(+)/GN, megalin deficient	5.03 ± 0.25	1.62 ± 0.13[c]	0.22 ± 0.05[c]	8.55 ± 0.27	1.18 ± 0.49	2.17 ± 0.66	30.67 ± 4.06[c]

[a]Data are means ± SD. Megalin-positive cells have a well-developed endosomal and lysosomal compartment that is lacking in megalin-deficient cells; this has little influence, however, on general cell height. In GN, megalin-positive cells show increased numbers of lysosomes compared with megalin-deficient cells. Basement membranes are thickened and mitochondrial volume is reduced in both variants as compared with controls without GN.

[b]$P < 0.05$, megalin-positive *versus* megalin-deficient cells.

[c]$P < 0.05$, control *versus* GN.

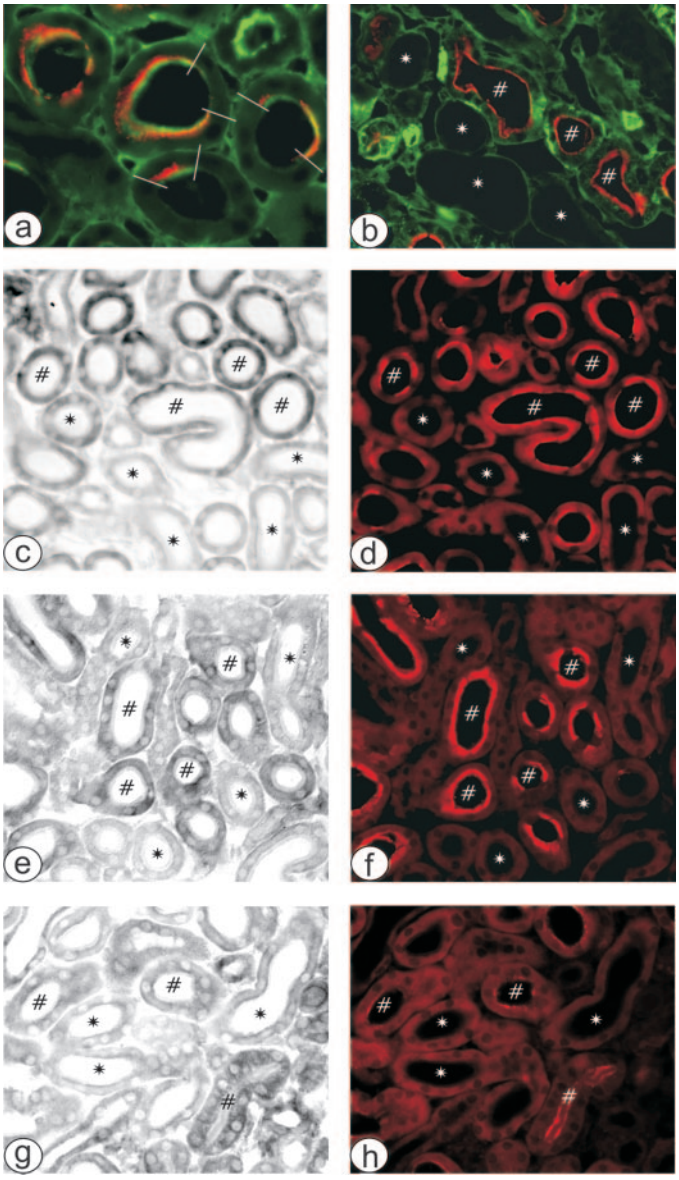

Figure 5. Histochemistry of inflammatory markers in Cre(+) mice with GN. (A) Double labeling of intercellular adhesion molecule-1 (ICAM-1; green) and megalin (red). ICAM-1–positive expression in brush border is mostly co-localized with megalin. White bars indicate the border between megalin-positive and megalin-deficient cells. (B) Double labeling of vascular cellular adhesion molecule-1 (VCAM-1; green immunofluorescence) and megalin (red immunofluorescence). Basolateral VCAM-1 expression mostly co-localizes with megalin (#), whereas there is no VCAM-1 staining in megalin-deficient proximal profiles (identified by interference contrast; *). (C and D) Double labeling of TGF-β1 mRNA expression (*in situ* hybridization; C) and megalin (red immunofluorescence; D). TGF-β1 mRNA was expressed in profiles where megalin was co-localized (#) but absent from megalin-deficient profiles (*). Similarly, TGF-β3 mRNA and megalin (E and F) and endothelin-1 mRNA and megalin (G and H) were mostly co-localized. Magnifications: ×200 in A; ×150 in B through H.

indication for a histotopographic association between protein endocytosis and inflammation or fibrosis.

Discussion

We used transgenic Cre(+) mice with kidney-specific megalin deficiency and control Cre(−) littermates to evaluate the effect of experimental GN and ensuing tubular protein overload on the development of tubulointerstitial disease. Symptoms of GN had developed in either genotype as previously established in rodent models (12,15,19–21). The Cre(+)/GN mice, however, unexpectedly presented a higher degree of glomerular as well as tubulointerstitial damage than the Cre(−)/GN mice.

The reason that Cre(+) mice reacted stronger to the experimental protocol than Cre(−) mice is not clear. However, pooling all Cre(+)/GN and Cre(−)/GN mice resulted in a strong positive correlation between glomerular and tubulointerstitial damage. This suggests that protein reabsorption has only a minor impact on the development of tubulointerstitial injury. However, the primary differences in disease manifestation among groups interfered with the interpretation of some of the data raised in Cre(+) as compared with Cre(−) mice. Therefore, the main emphasis in our study was put on intragroup comparisons between megalin-positive and megalin-deficient cells in the Cre(+)/GN group based on the mosaic remnant expression of megalin (14).

Structurally, changes in GN in both lines supported the previously established view that tubulointerstitial injury develops subsequent to the encroachment of a glomerular crescent onto the initial part of the proximal tubule (1,19). Tracing of the glomerulotubular junction in serial sections of Cre(+) and Cre(−) kidneys revealed that the affection of the initial proximal tubule in GN depended on the degree of the encroachment of the glomerular damage rather than on the presence or absence of megalin. The initial portion of the proximal tubule was structurally normal despite obvious protein leakage, as long as the glomerulotubular junction was patent. Conversely, more advanced encroachment of the crescents toward the tubule or obstruction were associated with degeneration and collapse of the tubule. Notably, this was independent of the expression of megalin as assessed by the occurrence or absence of an endocytic machinery in the tubular cells. This fits with previous experimental studies in rats and mice (19,20,22) as well as with findings in human disease, such as congenital nephrotic syndrome of the Finnish type (23), showing that heavy proteinuria does not necessarily induce tubular lesions.

As the second major finding, our results confirm that GN elicited an upregulation of the expression of ICAM-1, VCAM-1, TGF-β1, TGF-β3, ET-1, MCP-1, HSP25, and osteopontin, parameters that are known to be associated with proteinuria. In addition, the rates of cell proliferation and of apoptosis increased. Both the megalin-positive and the megalin-deficient segments were affected. Comparable changes were described previously (for a review, see reference [6]). However, because the development of tubulointerstitial disease in Cre(+)/GN mice with a majority of megalin-deficient proximal tubules obviously followed the same pattern as in Cre(−)/GN mice

Figure 6. Histochemistry of osteopontin (A and B) and heat shock protein 25 (HSP25) expression (C) in Cre(+) mice with GN. (A and B) Osteopontin mRNA (*in situ* hybridization; A) and megalin (#; brown immunoperoxidase staining; B) in consecutive sections mostly show mutually exclusive labeling with osteopontin mRNA expressed in megalin-deficient proximal tubules (*). Black bars indicate border between megalin-positive, osteopontin-negative and megalin-deficient, osteopontin-positive portions within the same tubule. (C) Double labeling of HSP25 (green immunofluorescence) and megalin (red immunofluorescence). Proximal tubule portions mostly show mutually exclusive staining for HSP25 (*) or megalin (#). White bars indicate border between megalin-positive, HSP25-negative and megalin-deficient, HSP25-positive portions within the same tubule. Magnification, ×150.

Table 3. Cell-cycle data[a]

Parameter	Cre(+)/Control Megalin-Positive Cells	Cre(+)/Control Megalin-Deficient Cells[b]	Cre(+)/GN Megalin-Positive Cells[c]	Cre(+)/GN Megalin-Deficient Cells[b,c]
Ki-67	6.9×10^{-5}	3.9×10^{-4}	3.4×10^{-2}	1.5×10^{-2}
PCNA	1.0×10^{-4}	3.6×10^{-4}	6.3×10^{-2}	3.7×10^{-2}
Apoptosis	6.1×10^{-4}	1.5×10^{-3}	9.6×10^{-2}	2.4×10^{-1}

[a]Megalin-positive and megalin-deficient cells of the proximal tubules of Cre(+) groups are compared. The numbers of positive nuclei per total proximal tubule nuclei are indicated.
[b]$P < 0.05$, megalin-positive *versus* megalin-deficient cells.
[c]$P < 0.05$, control *versus* GN.

with normal proximal tubules, the role of the protein overload hypothesis may be questioned. Because the inflammatory parameters did not coincide with the tubulointerstitial injury, their commonly assumed pathogenetic role could in fact be different. This raises the question as to the relevance of their upregulation.

It is known that ICAM-1, VCAM-1, and ET-1 have several potential binding sites for NF-κB in their promoter region and that binding of NF-κB may be relevant for their activation (24–28). Substantial protein uptake in cultured cells also induced signaling *via* NF-κB (for review, see reference [29]). It is therefore reasonable to assume that in GN, the expression of ICAM-1, VCAM-1, and ET-1 within tubular cells reflects the activation of NF-κB. In renal pathophysiology, NF-κB–mediated responses are often considered pathogenic (29). However, there is also good evidence that NF-κB may mediate protective cellular adaptation to stress and also prevent apoptosis (30,31).

Similarly, TGF-β is generally considered to play a pivotal role in renal pathology regarding fibrogenesis and scarring (32), yet increased collagen expression in our model was not specifically associated with the upregulated TGF-β transcripts. TGF-β isoforms are considered to be multifunctional, and recent work emphasized the dosage dependence of their effects; in glomerular epithelial cells, a critical TGF-β concentration threshold that specifies a molecular switch from growth arrest/differentiation to proapoptotic signaling and apoptosis was found (33). In line with this, lower dosages of TGF-β promoted neurogenesis within ganglia, whereas slightly higher dosages induced apoptosis (34). Therefore, it may be suggested that the TGF-β–mRNA increases in response to enhanced protein uptake were insufficient to initiate deleterious effects. Rather, we speculate that the increases represented a protective response to stress, apparently including diminished susceptibility to proapoptotic signals in Cre(+)/GN.

Consequently, we assume that in GN, increased protein uptake by megalin-positive cells induces an anti-stress response that includes augmented expression of ICAM-1, VCAM-1, TGF-β1, TGF-β3, and ET-1, which along with selectively enhanced cell proliferation may serve protective rather than pathologic functions. Regarding the increased rate of apoptosis in megalin-deficient compared with megalin-positive cells, we therefore suggest that megalin-deficient cells, which lack the protective stress response that is elicited by protein uptake, may have an increased susceptibility to undefined stimuli of disease progression in our model. A study by Erkan *et al.* (35) supports the view that apoptosis might be caused by stimuli other than protein overload, because there was enhanced apoptosis in kidneys with FSGS and membranoproliferative GN but not in kidneys with minimal-change disease. Reactive oxygen species

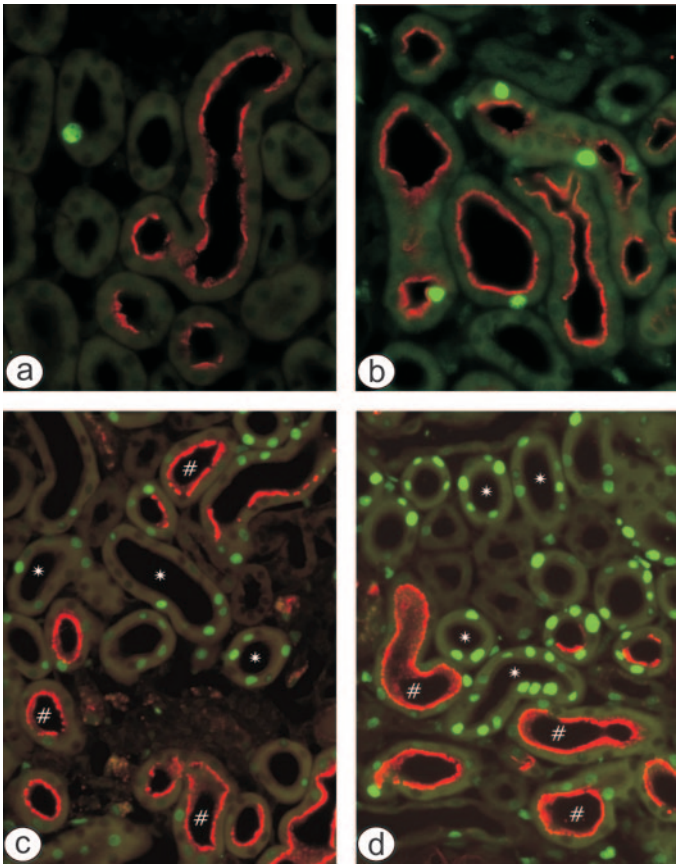

Figure 7. Histochemical markers for cell proliferation (Ki-67; green) and apoptosis (terminal deoxynucleotidyl transferase–mediated digoxigenin-deoxyuridine nick-end labeling [TUNEL]; green) in control Cre(+) (A and C) and Cre(+)/GN (B and D). Sections are double stained for megalin (red). (A) Baseline Ki-67 signal in a megalin-deficient proximal tubule profile. (B) Enhanced Ki-67 signal is localized preferentially in megalin-positive proximal tubule profiles. (C and D) TUNEL signals in both conditions are mainly found in megalin-deficient profiles; note the increased signal in GN (D). Magnification, ×150.

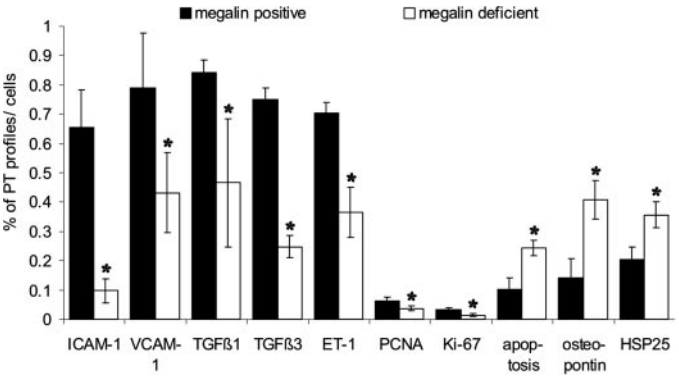

Figure 8. Quantification of histochemical data. Numerical evaluation of proximal tubular profiles is presented except for VCAM-1 immunoreactivity, proliferation, and apoptosis, where single VCAM-1–, PCNA-, Ki-67–, or TUNEL-positive cells located in megalin-positive or in megalin-deficient proximal tubule profiles have been counted. Data are means ± SD. *$P < 0.05$.

may as well menace the intactness of the proximal tubule (36), but this issue has also been discussed controversially (37–39).

It may also be considered that altered intracellular supply of potentially vital small molecules to the proximal tubule, caused by the disrupted endocytosis, could have proapoptotic influence to contribute to the selective increase of TUNEL signal of megalin-deficient cells in GN. As yet, there is no basis for a speculation about the possible role of such molecules in GN, but a recent article suggested another pathway for regulation of stress responses *via* megalin (40). It was found that megalin binds to and activates protein kinase B (Akt). Activated Akt promotes cell survival, partly *via* NF-κB, and inhibits apoptosis.

An enhanced expression of the stress-related products osteopontin and HSP25 was also found preferentially in megalin-

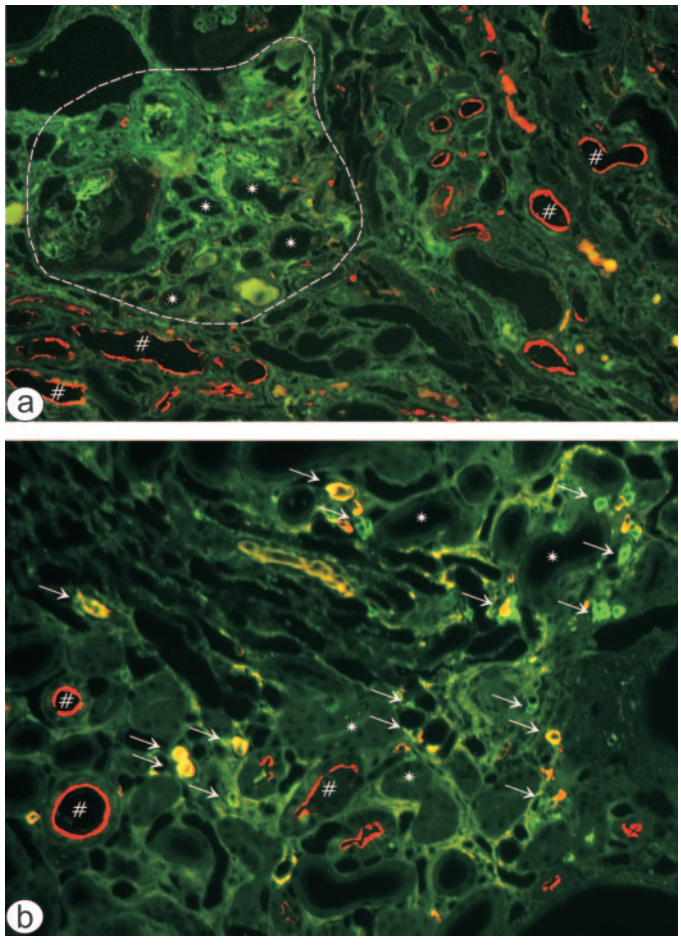

Figure 9. Histochemistry of interstitial parameters in Cre(+) mice with GN. (A) Double labeling of collagen I (green) and megalin (red immunofluorescence). Collagen I is predominantly expressed in areas of glomerular and tubular degeneration. Of note, collagen I was mostly in close proximity to megalin-deficient (*) rather than to megalin-positive proximal tubule profiles (#). (B) Double labeling of macrophage marker CD68 (green/yellow immunofluorescence; arrows) and megalin (red). CD68-positive macrophages (individual cells or clusters of cells) are localized to fibrotic areas and to the vicinity of megalin-deficient (*) rather than to megalin-positive proximal tubule profiles (#). Magnification, ×90.

deficient PTP in GN. Because upregulation of both products was further observed in distal tubules, displaying only minor protein uptake (37), changes likely did not depend on protein overload; notably, their upregulation correlated with the increased apoptosis rate in megalin-deficient cells ($r = 0.925$ for osteopontin and $r = 0.975$ for HSP25).

Conclusions

Our data suggest that excessive uptake of filtered proteins by proximal tubules has no major impact on the development of the tubulointerstitial disease in GN. Upregulation of inflammatory proteins in response to excessive protein uptake may represent a stress-protective function rather than a disease-inducing mechanism. Instead, our results support the view that expanding damages at the glomerulotubular junction represent the crucial moment in the transmission of the disease from the glomerulus to the tubule.

Acknowledgments

This project was supported by the Deutsche Forschungsgemeinschaft (FG 406, FOR 667).

We thank Rolf Nonnenmacher for help with the illustrations and Pascale Schulte for manuscript editing.

Disclosures

None.

References

1. Kriz W, Le Hir M: Pathways to nephron loss starting from glomerular diseases: Insights from animal models. *Kidney Int* 67: 404–419, 2005
2. Couser WG: Pathogenesis of glomerulonephritis. *Kidney Int Suppl* 42: S19–S26, 1993
3. Burton C, Harris KP: The role of proteinuria in the progression of chronic renal failure. *Am J Kidney Dis* 27: 765–775, 1996
4. Remuzzi G, Bertani T: Pathophysiology of progressive nephropathies. *N Engl J Med* 339: 1448–1456, 1998
5. Keane WF: Proteinuria: Its clinical importance and role in progressive renal disease. *Am J Kidney Dis* 35[Suppl 1]: S97–S105, 2000
6. Zoja C, Morigi M, Remuzzi G: Proteinuria and phenotypic change of proximal tubular cells. *J Am Soc Nephrol* 14[Suppl 1]: S36–S41, 2003
7. Christensen EI, Birn H: Megalin and cubilin: Multifunctional endocytic receptors. *Nat Rev Mol Cell Biol* 3: 256–266, 2002
8. Nykjaer A, Dragun D, Walther D, Vorum H, Jacobsen C, Herz J, Melsen F, Christensen EI, Willnow TE: An endocytic pathway essential for renal uptake and activation of the steroid 25-(OH) vitamin D3. *Cell* 96: 507–515, 1999
9. Dixon R, Brunskill NJ: Activation of mitogenic pathways by albumin in kidney proximal tubule epithelial cells: Implications for the pathophysiology of proteinuric states. *J Am Soc Nephrol* 10: 1487–1497, 1999
10. Tang S: Transferrin but not albumin mediates stimulation of complement C3 biosynthesis in human proximal tubular epithelial cells. *Am J Kidney Dis* 37: 94–103, 2001
11. Gross ML, Hanke W, Koch A, Ziebart H, Amann K, Ritz E: Intraperitoneal protein injection in the axolotl: The amphibian kidney as a novel model to study tubulointerstitial activation. *Kidney Int* 62: 51–59, 2002
12. Benigni A, Corna D, Zoja C, Longaretti L, Gagliardini E, Perico N, Coffman TM, Remuzzi G: Targeted deletion of angiotensin II type 1A receptor does not protect mice from progressive nephropathy of overload proteinuria. *J Am Soc Nephrol* 15: 2666–2674, 2004
13. Leheste JR, Melsen F, Wellner M, Jansen P, Schlichting U, Renner-Müller I, Andreassen TT, Wolf E, Bachmann S, Nykjaer A, Willnow TE: Hypocalcemia and osteopathy in mice with kidney-specific megalin gene defect. *FASEB J* 17: 247–249, 2003
14. Bachmann S, Schlichting U, Geist B, Mutig K, Petsch T, Bacic D, Wagner CA, Kaissling B, Biber J, Murer H, Willnow T: Kidney-specific inactivation of the megalin gene impairs trafficking of renal inorganic sodium phosphate-cotransporter (NaPi-IIa). *J Am Soc Nephrol* 15: 892–900, 2004
15. Le Hir M, Haas C, Marino M, Ryffel B: Prevention of crescentic glomerulonephritis induced by anti-glomerular membrane antibody in tumor necrosis factor-deficient mice. *Lab Invest* 78: 1625–1631, 1998
16. Theilig F, Bostanjoglo M, Pavenstadt H, Grupp C, Holland G, Slosarek I, Gressner AM, Russwurm M, Koesling D, Bachmann S: Cellular distribution and function of soluble guanylyl cyclase in rat kidney and liver. *J Am Soc Nephrol* 12: 2209–2220, 2001
17. Ma LJ, Nakamura S, Whitsitt JS, Marcontoni C, Davidson JM, Fogo AB: Regression of sclerosis in aging by an angiotensin inhibition-induced decrease in PAI-1. *Kidney Int* 58: 2425–2436, 2000
18. Kaissling B, Stanton BA: Adaptation of distal tubule and collecting duct to increased sodium delivery. I. Ultrastructure. *Am J Physiol* 255: F1256–F1268, 1988
19. Le Hir M, Besse-Eschmann V: A novel mechanism of nephron loss in a murine model of crescentic glomerulonephritis. *Kidney Int* 63: 591–599, 2003
20. Kriz W, Hahnel B, Hosser H, Ostendorf T, Gaertner S, Kranzlin B, Gretz N, Shimizu F, Floege J: Pathways to recovery and loss of nephrons in anti-Thy-1 nephritis. *J Am Soc Nephrol* 14: 1904–1926, 2003
21. Le Hir M, Keller C, Eschmann V, Hahnel B: Hosser H, Kriz W: Podocyte bridges between the tuft and Bowman's capsule: An early event in experimental crescentic glomerulonephritis. *J Am Soc Nephrol* 12: 2060–2071, 2001
22. Kriz W, Hartmann I, Hosser H, Hahnel B, Kranzlin B, Provoost A, Gretz N: Tracer studies in the rat demonstrate misdirected filtration and peritubular filtrate spreading in nephrons with segmental glomerulosclerosis. *J Am Soc Nephrol* 12: 496–506, 2001
23. Kuusniemi AM, Lapatto R, Holmberg C, Karikoski R, Rapola J, Jalanko H: Kidneys with heavy proteinuria show fibrosis, inflammation, and oxidative stress, but no tubular phenotypic change. *Kidney Int* 68: 121–132, 2005
24. Roebuck KA, Finnegan A: Regulation of intercellular adhesion molecule-1 (CD54) gene expression. *J Leukoc Biol* 66: 876–888, 1999
25. Iademarco MF, McQuillan JJ, Rosen GD, Dean DC: Characterization of the promoter for vascular cell adhesion molecule-1 (VCAM-1). *J Biol Chem* 26: 16323–16329, 1992
26. Kuldo JM, Westra J, Asgeirsdottir SA, Kok RJ, Oosterhuis K, Rots MG, Schouten JP, Limburg PC, Molema G: Differ-

ential effects of NF-kappaB and p38 MAPK inhibitors and combinations thereof on TNF-alpha- and IL-1beta-induced proinflammatory status of endothelial cells in vitro. *Am J Physiol Cell Physiol* 289: C1229–C1239, 2005
27. Collins T, Read MA, Neish AS, Whitley MZ, Thanos D, Maniatis T: Transcriptional regulation of endothelial cell adhesion molecules: NF-kappa B and cytokine-inducible enhancers. *FASEB J* 9: 899–909, 1995
28. Park JY, Kim YM, Song HS, Park KY, Kim YM, Kim MS, Pak YK, Lee IK, Lee JD, Park SJ, Lee KU: Oleic acid induces endothelin-1 expression through activation of protein kinase C and NF-kappa B. *Biochem Biophys Res Commun* 303: 891–895, 2003
29. Zoja C, Benigni A, Remuzzi G: Cellular responses to protein overload: Key event in renal disease progression. *Curr Opin Nephrol Hypertens* 13: 31–37, 2004
30. Yang CH, Murti A, Pfeffer SR, Basu L, Kim JG, Pfeffer LM: IFNalpha/beta promotes cell survival by activating NF-kappa B. *Proc Natl Acad Sci U S A* 97: 13631–13636, 2000
31. Chen F, Bower J, Leonard SS, Ding M, Lu Y, Rojanasakul Y, Kung HF, Vallyathan V, Castranova V, Shi X: Protective roles of NF-kappa B for chromium(VI)-induced cytotoxicity is revealed by expression of Ikappa B kinase-beta mutant. *J Biol Chem* 277: 3342–3349, 2002
32. Yu L, Border WA, Huang Y, Noble NA: TGF-isoforms in renal fibrogenesis. *Kidney Int* 64: 844–856, 2003
33. Wu DT, Bitzer M, Ju W, Mundel P, Bottinger EP: TGF-beta concentration specifies differential signaling profiles of growth arrest/differentiation and apoptosis in podocytes. *J Am Soc Nephrol* 16: 3211–3221, 2005
34. Hagedorn L, Floris J, Suter U, Sommer L: Autonomic neurogenesis and apoptosis are alternative fates of progenitor cell communities induced by TGFbeta. *Dev Biol* 228: 57–72, 2000
35. Erkan E, Garcia CD, Patterson LT, Mishra J, Mitsnefes MM, Kaskel FJ, Devarajan P: Induction of renal tubular cell apoptosis in focal segmental glomerulosclerosis: Roles of proteinuria and fas-dependent pathways. *J Am Soc Nephrol* 16: 398–407, 2005
36. Iglesias J, Abernethy VE, Wang Z, Lieberthal W, Koh JS, Levine JS: Albumin is a major serum survival factor for renal tubular cells and macrophages through scavenging of ROS. *Am J Physiol Renal Physiol* 277: F711–F722, 1999
37. Erkan E, Devarajan P, Schwartz GJ: Apoptotic response to albumin overload: Proximal vs. distal/collecting tubule cells. *Am J Nephrol* 25: 121–131, 2005
38. Thomas ME, Brunskill NJ, Harris KPG, Bailey E, Pringle JH, Furness PN, Walls J: Proteinuria induces tubular cell turnover: A potential mechanism for tubular atrophy. *Kidney Int* 55: 890–898, 1999
39. Benigni A, Gagliardini E, Remuzzi A, Corna D, Remuzzi G: Angiotensin-converting enzyme inhibition prevents glomerular-tubule disconnection and atrophy in passive Heymann nephritis, an effect not observed with a calcium antagonist. *Am J Pathol* 159: 1743–1750, 2001
40. Caruso-Neves C, Pinheiro AAS, Cai H, Souza-Menezes J, Guggino WB: PKB and megalin determine the survival or death of renal proximal tubule cells. *Proc Natl Acad Sci U S A* 103: 18810–18815, 2006

See the related editorial, "More on Renal Disease Progression: Is Interstitial Inflammation Truly Protective," on pages 1630–1632.